The role of halogens in polychlorotrifluoroethylene (PCTFE) in membrane gas separations

Milad Yavari[a], Yoshiyuki Okamoto[b], Haiqing Lin[a],[*]

[a] *Department of Chemical and Biological Engineering, University at Buffalo, The State University of New York, Buffalo, NY 14260, USA*
[b] *Department of Chemical and Biomolecular Engineering, Tandon School of Engineering, New York University, Six MetroTech Center, Brooklyn, NY 11201, USA*

ARTICLE INFO

ABSTRACT

Halogenated polymers have emerged as interesting materials for membrane gas separation. Herein, we demonstrate that a combination of F and Cl substituents in polymers provide unexpectedly superior He/gas separation properties, as exemplified by polychlorotrifluoroethylene (PCTFE). PCTFE exhibits a He permeability of 26 Barrers at 35 °C and pure gas selectivity of He/H_2, He/CO_2, and He/CH_4 of 6.2, 53, and 1100, respectively. These selectivity values are among the highest reported for polymers, and the separation performance is very close to the Robeson's upper bounds. The effect of crystallinity in PCTFE on gas transport properties is discussed, and the gas transport properties in PCTFE are compared with other polyethylene (PE) analogues such as PE, polyvinyl chloride (PVC), polyvinylidene fluoride (PVDF), and polytetrafluoroethylene (PTFE). The effect of F and Cl substituents on gas solubility is also elucidated using a variety of hydrocarbons and halogenated liquids. The F substituents lead to unexpectedly high He solubility and exhibit unfavorable interactions with H_2 and CH_4, while the Cl substituents increase solubility parameter and size-sieving ability, both of which contribute to the superior He/gas separation properties (particularly He/H_2 and He/CH_4). The understanding of the role of F and Cl substituents of polymers in gas transport properties can be useful in designing high performance polymers for membrane gas separation.

1. Introduction

Polymers with high gas permeability and selectivity are of great interests for membrane gas separation, an energy-efficient gas separation technology [1–3]. However, there is a trade-off between gas permeability and selectivity, i.e., polymers with higher permeability exhibit lower selectivity, and vice versa [4–6]. Such a trade-off is ascribed to an intrinsic dilemma that polymers with higher free volume exhibit higher permeability but weaker size-sieving ability and thus lower selectivity [7,8]. An effective strategy to design polymers overcoming the trade-off is to incorporate functional groups that interact with gases, increasing solubility selectivity and thus permeability selectivity without significantly decreasing permeability [5,6,9–12].

Halogenated polymers have demonstrated interesting gas separation properties [13–19]. For example, perfluoropolymers have unfavorable interactions with hydrocarbons such as CH_4 and thus, they have been considered for N_2/CH_4 and CO_2/CH_4 separation [4,15,16,20,21], and they have unexpectedly high helium solubility, resulting in high He/N_2 and He/CH_4 separation performance [20–23]. The upper bounds for N_2/CH_4, He/H_2 and He/CH_4 separation in the

Robeson's plots are governed by the amorphous glassy perfluoropolymers such as Hyflon® AD and Teflon® AF, which are copolymers of tetrafluoroethylene (TFE) and perfluorodioxlanes [4,20,21]. The TFE component provides high selectivity of He/CH_4 and He/H_2, while the perfluorodioxlane disrupts the TFE crystallization and provides high gas permeability. Recently, a series of copolymers of chlorotrifluoroethylene (CTFE) and perfluoro(2-methylene-4,5-dimethyl-1,3-dioxolane) (PFMDD) have been synthesized, and exhibit superior He/CH_4 and CO_2/CH_4 separation properties [20,21]. For example, a copolymer comprising 30% CTFE and 70% PFMDD shows He/CH_4 and CO_2/CH_4 selectivity of 480 and 48, respectively, which is very attractive for practical separations [24].

Despite the success in exploring these fluoropolymers for membrane gas separation, there lacks systematic understanding of gas transport properties in the polymers containing Cl and F substituents. In this work, we selected polychlorotrifluoroethylene (PCTFE) to elucidate the effect of F and Cl substituents on gas transport properties. There are few data on gas transport in PCTFE in the literature, though it is commercially available [25]. We systematically determine physical properties of PCTFE (including crystallinity and fractional free volume) and

* Corresponding author.
  E-mail address: haiqingl@buffalo.edu (H. Lin).

examine the effect of fluorine and chlorine groups on membrane gas separation properties. The effect of F and Cl on gas solubility is also elucidated using exampled halogenated organic liquids. Surprisingly, this simple polymer containing both F and Cl substituents demonstrates great potential for He/gas and H_2/CO_2 separation. Understanding the role of F and Cl substituents in the structure/gas separation property relationship is valuable to design advanced polymers with superior gas separation properties.

2. Experimental section

2.1. Materials

Thin films of PCTFE (under the tradename of HydroBlock® P600TR) were generously provided by Honeywell Performance Materials and Technologies (Pottsville, PA). Gas cylinders of N_2, Ar, H_2 and He with a purity of 99.999%, CH_4 and CO_2 (99.9%), and C_2H_6 (99.3%) were obtained from Praxair, Inc. (Tonawanda, NY).

2.2. Characterization of physical properties of PCTFE films

Density and thickness of the PCTFE films were determined using the geometric method. The weight was measured by an analytical balance, Model XS 64 (Mettler-Toledo, Columbus, OH), and the volume was determined using Accu-Pyc II 1340 Gas Pycnometer (Micromeritics Instrument Corporation, Norcross, GA). Films of about 0.3 g were used to achieve high accuracy of the volume measurement. Because the commercial films have uniform thickness, the thickness is calculated from the volume and known surface area.

An Ultima IV X-ray diffractometer (Rigaku Corporation, Tokyo, JP) with CuKα radiation (with a wavelength of 1.54 Å) was used to characterize the PCTFE films at a scanning range of $5 - 50°$ and a scanning rate of 0.5°/min. The obtained Wide-angle X-Ray Diffraction (WAXD) spectra were analyzed using Rigaku PDXL software 4.2.2 to estimate the crystallinity.

Differential scanning calorimetry (DSC, Q2000, TA Instruments, New Castle, DE) was used to determine thermal transitions of the PCTFE films. The measurement was performed at a heating rate of 10 °C/min from 25 °C to 250 °C under a nitrogen gas flow of 50 ml/min. Universal Analysis 2000 software was used to determine glass transition temperature (T_g), melting temperature (T_m), and heat of crystallization and melting.

2.3. Determination of pure-gas permeation and sorption properties

Pure-gas permeability of CH_4, N_2, Ar, CO_2, H_2, and He through PCTFE films was determined using a constant volume/variable pressure apparatus at 35 °C [26,27]. A PCTFE film masked using an aluminum tape with an active area of 2.0 cm^2 was mounted in a permeation cell (Millipore Corporation, Bedford, MA). The steady-state rate of pressure increase in the downstream with a known volume was used to calculate gas permeability. Gas permeability (P_A) has units of Barrers, where 1 Barrer = 10^{-10} cm^3(STP) cm/(cm^2 s cmHg).

Pure-gas solubility of CH_4, Ar, CO_2 and C_2H_6 in PCTFE films was determined using a dual-volume and dual-transducer apparatus based on a pressure decay method [26,28]. Polymer films were placed in a sample cell and evacuated overnight. A known amount of gas was then introduced into the sample cell, and the pressure in the sample cell decreased due to the gas sorption by the polymer. The gas solubility (S_A) can be calculated using the following equation:

$$S_A = C_A/p_A \tag{1}$$

where C_A is the concentration of the sorbed gas (cm^3 (STP)/cm^3 polymer) in the polymer at an equilibrium pressure of p_A (atm). The determined solubility of CH_4, Ar, CO_2 and C_2H_6 has an uncertainty less than 10%, which was estimated based on error propagation and

analysis [29]. The sorption of He, H_2 and N_2 was too low to determine using this method [26].

Within the framework of the solution-diffusion mechanism, gas diffusivity (D_A, cm^2/s) in PCTFE can be calculated using the following equation [30]:

$$D_A = P_A/S_A \tag{2}$$

3. Results and discussion

3.1. Fractional free volume and crystallinity in PCTEF

Gas transport properties in polymers are influenced by polymer morphology, such as fractional free volume (*FFV*) [31] and crystallinity in volume percentage (φ_c) [28,32,33]. The *FFV* of the amorphous phase polymer can be estimated using the following equation [31,34]:

$$FFV = 1 - \rho_a V_o \tag{3}$$

where ρ_a is the density of amorphous PCTFE, and V_o is the specific occupied volume at 0 K, which can be estimated as 1.3 times of van der Waals volume [34]. Based on a value of 2.077 g/cm^3 for ρ_a [35], the *FFV* in PCTFE is estimated to be 0.170.

Polymer crystallinity can be estimated using three methods, i.e., density, heat of melting from the DSC, and WAXD spectrum [28]. The φ_c values from these three methods are described below.

First, the φ_c can be estimated from the polymer density (ρ_P) using Eq. (4) [28]:

$$\varphi_c = \frac{\rho_P - \rho_a}{\rho_c - \rho_a} \times 100\% \tag{4}$$

where ρ_c is the density of crystalline phase (2.187 g/cm^3) [35]. Based on the density value of 2.137 g/cm^3 determined from the geometric method in this study, the φ_c has a value of 54%.

Second, the φ_c can be estimated from the DSC curve shown in Fig. 1. As temperature increases from 25 °C to 250 °C, the polymer exhibits a T_g of 63 °C, a crystallization peak at 89 °C, and a melting peak at 211 °C. These thermal transitions are consistent with those reported in the literature [36–38].

The φ_c value can be estimated from the heat of melting using the following equation [28,39,40]:
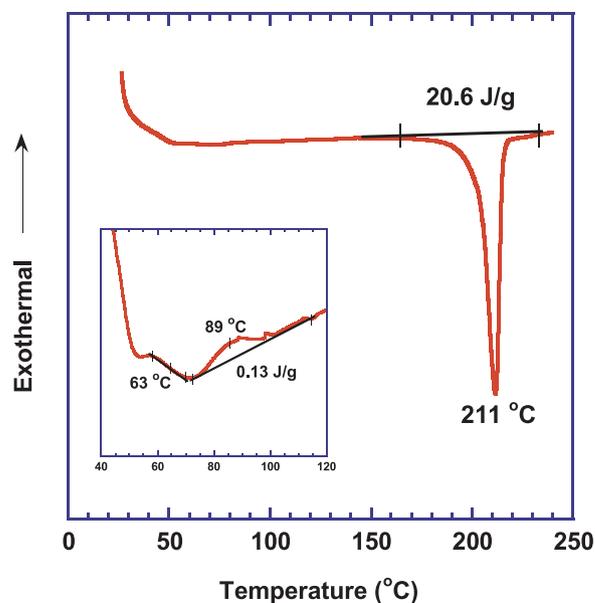

Fig. 1. The first heating scan of DSC thermogram for PCTFE films. The inset shows the thermal transitions of T_g and crystallization.
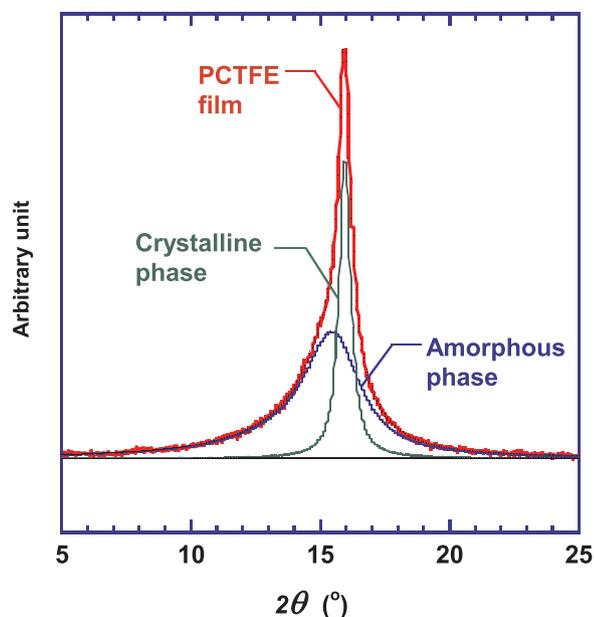
Fig. 2. WAXD spectrum of the PCTFE film. The peak at the 2θ value of 16° is de-convoluted to the crystalline and amorphous phase.

$$\varphi_c = \frac{(\Delta H_m - \Delta H_c)}{\Delta H_m^{100\%}} \frac{\rho_P}{\rho_c} \qquad (5)$$

where ΔH_m is the melting enthalpy at 211 °C (20.6 J/g), ΔH_c is the crystallization enthalpy at 89 °C (0.13 J/g), and $\Delta H_m^{100\%}$ is the melting enthalpy of 100% crystalline PCTFE. With a $\Delta H_m^{100\%}$ value of 40 ± 5 J/g for PCTFE [38], the obtained φ_c value is 50 ± 6%, which is consistent with that obtained from the density measurement.

Finally, the crystallinity can also be determined from the WAXD spectrum, as shown in Fig. 2. The PCTFE crystals have characteristic peaks at 2θ values of 16.0° (101), 16.4° (102), 17.0° (103), and 18.0° (104), and the amorphous PCTFE has a halo at a 2θ value of 16° [35]. The spectrum can be de-convoluted to the amorphous and crystalline phase using the Pseudo-Voigt approximation method and Rigaku PDXL XRD analysis software, where the sharp and broad peak correspond to the crystalline and amorphous phase, respectively [40]. The weight percentage crystallinity is calculated by the area ratio of crystals peaks
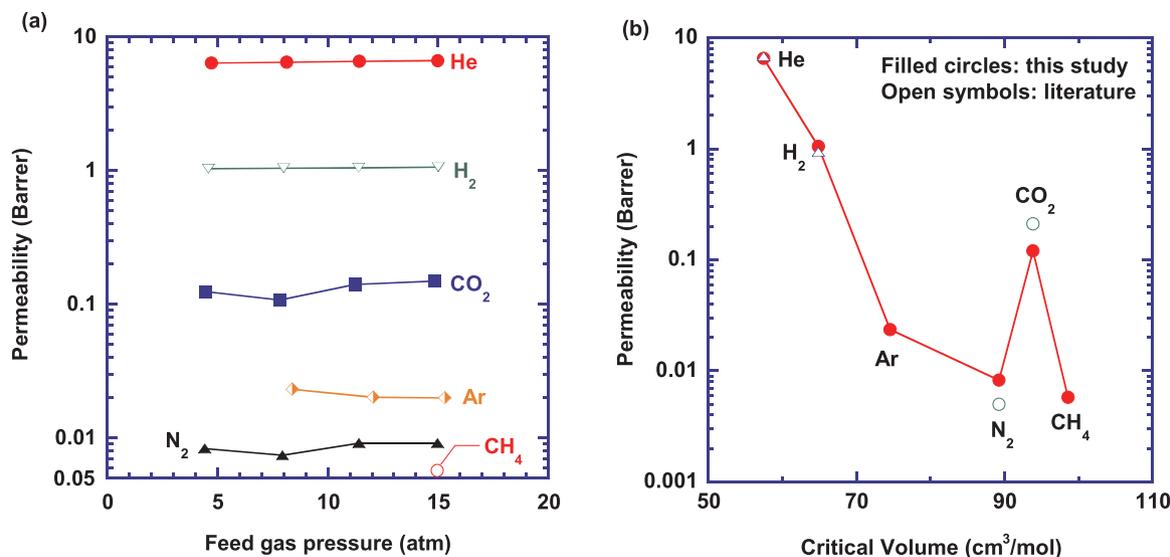
Table 1
Critical temperature (T_c), critical volume (V_c), and polarizability (α) for relevant gases studied in this work [44].

Gas	T_c (K)	V_c (cm^3/mol)	$\alpha \times 10^{24}$ (cm^3)
He	5.2	57.5	0.205
Ne	44	41.9	0.394
H_2	33	64.4	0.80
O_2	154	73.4	1.57
Ar	132	74.6	1.64
N_2	126	89.4	1.74
Kr	209	92.2	2.48
CH_4	190	98.6	2.59
CO_2	304	94.1	2.91
C_2H_6	305	147	4.47

to all peaks and halos, which yields a value of 40% for φ_c.

To summarize, the φ_c values for the PCTFE film are 54%, 50%, and 40% based on the density, DSC and XRD results, respectively. These values are more or less consistent, considering the vastly different mechanisms [28]. In the following analysis, the φ_c value (50%) from the DSC result is used, since the DSC is the most widely used approach for crystallinity measurement among these methods.

3.2. Gas permeability of PCTFE

Fig. 3a presents pure-gas permeability of CH_4, N_2, Ar, CO_2, H_2 and He in PCTFE films at 35 °C as a function of feed pressure. The CH_4 permeability was only determined at 15 atm, because the gas flux at lower pressures was too low to measure. For all other gases except CO_2, permeability is almost independent of the feed pressure, indicating that the film is defect-free. CO_2 permeability slightly increases with increasing pressure, due to the plasticization of the polymer by the sorbed CO_2 [8,41]. Fig. 3b shows the gas permeability as a function of critical volume of gas molecules (as summarized in Table 1). Gas permeability decreases with increasing the critical volume or penetrant size, which is typical for glassy polymers with strong size-sieving ability. Fig. 3b also compares the gas permeability obtained in this work with those reported in the literature [42,43], where the measurements were performed with few gases at different temperatures, and the polymer crystallinity may not be reported [42]. As shown in Fig. 3b, there is a good consistency in He and H_2 permeability between this work and the literature [42], while this study yields higher N_2 permeability and

Fig. 3. Pure gas permeability of the PCTFE film at 35 °C as a function of (a) feed pressure, and (b) critical volume of gas molecules. In (b), the symbol of ● represents the permeability at 7.8 atm from this work, the symbol of Δ represents the permeability at 20 °C in PCTFE with an unknown crystallinity [42], and the symbol of ○ represents the permeability of N_2 at 25 °C and CO_2 at 40 °C in PCTFE (Kel-F 300 with a crystallinity of ~30%) [43].

Table 2
Estimated amorphous-phase gas permeability ($P_{A,am}$) and He/gas selectivity ($\alpha_{He/gas}$) in PCTFE at 35 ˚C, compared with those in amorphous PE and PTFE at 25 ˚C.

Gas	PCTFE		PE[a]		PTFE[b]	
	$P_{A,am}$ (Barrers)	$\alpha_{He/gas}$	$P_{A,am}$ (Barrers)	$\alpha_{He/gas}$	$P_{A,am}$ (Barrers)	$\alpha_{He/gas}$
CH_4	0.023	1100	8.9	1.7	0.76	16
N_2	0.033	790	3.0	5.0	1.4	8.6
Ar	0.094	280	8.4	1.8	2.0	6
CO_2	0.48	53	38	0.4	11.5	1.0
H_2	4.2	6.2	–	–	9.6	1.2
He	26		15		12	

[a] Alathon 14 from [48].
[b] He, H_2, Ar and CH_4 permeability are from [46], and CO_2 and N_2 permeability are from [47].

lower CO_2 permeability than those in the literature, presumably due to the difference in the testing temperatures and polymer morphology such as crystallinity [43].

In semi-crystalline polymers, the crystalline phase is often inaccessible to penetrants, and thus, gas sorption and diffusion only occur in the amorphous phase. The following simple models can be used to estimate gas transport properties in the amorphous phase [28,32,33]:

$$S_{A,SC} = S_{A,am} \times \varphi_{am} \qquad (6)$$

$$P_{A,SC} = P_{A,am} \times \varphi_{am}^2 \qquad (7)$$

where φ_{am} is the volume fraction of the amorphous phase in the polymer, and the subscripts of *SC* and *am* indicate the properties of semi-crystalline and amorphous polymers, respectively. The amorphous-phase diffusivity ($D_{A,am}$) can be calculated as the ratio of $P_{A,am}$ to $S_{A,am}$. In this study, the φ_{am} is 50% in PCTFE, since φ_c equals to 50%.

Table 2 records the estimated permeability of amorphous phase PCTFE and He/gas selectivity at 7.8 atm and 35 ˚C, which are compared with those in an amorphous hydrocarbon analogue (polyethylene, PE) and perfluoropolymer analogue (polytetrafluoroethylene, PTFE). PCTFE exhibits lower gas permeability than PE and PTFE, except for He. More importantly, PCTFE shows unusually high He/gas selectivity, compared with its hydrocarbon and perfluoropolymer analogue. For example, the CO_2/N_2 selectivity in PCTFE is 14, comparable to 12 in PE and 8.2 in PTFE [45–47]. On the other hand, the He/gas selectivity in PCTFE is one to two orders magnitude higher than that in PE and PTFE.

Interestingly, PCTFE also shows a H_2/CO_2 selectivity of 8.5 at 35 ˚C, an attractive performance for H_2 purification and CO_2 capture. The details will be discussed in Section of Superior gas separation performance of PCTFE.

3.3. Gas solubility and diffusivity in PCTFE

Fig. 4a presents sorption isotherms of CH_4, Ar, C_2H_6 and CO_2 in the PCTFE at 35 ˚C. The isotherms for CO_2 and C_2H_6 are slightly concave due to the Langmuir sorption [49]. For simplicity, these sorption data are fitted using the Henry's law (as shown in Eq. (1)). In general, gas solubility increases with increasing condensability (as indicated by critical temperature). Fig. 4b exhibits the gas diffusivity in the amorphous phase PCTFE as a function of penetrant critical volume. As expected, gas diffusivity decreases with increasing penetrant critical volume.

Table 3 compares physical properties in PCTFE with representative fluorinated and chlorinated PE analogues, such as solubility parameter (δ_P) and T_g. Asymmetric substitutions of F and Cl in PE increases both δ_P and T_g. For example, introducing F and Cl substituents to PE increases T_g to -40 ˚C in PVDF) and 71 ˚C in PVC, respectively [52], and the introduction of Cl in PTFE increases the δ_P (from 12.7 to 15.7 MPa$^{0.5}$) and T_g (from -110 to 63 ˚C) in PCTFE. As shown in Fig. 4b, the $D_{A,am}$ values follow the order of PE > PTFE > PVDF > PVC ≈ PCTFE, which is almost the same as the increasing order of T_g, except PE. In general, as polymer chains become more rigid (as indicated by higher T_g), it becomes more difficult for polymer chains to open up a gap for gas molecule to diffuse and thus, gas diffusivity decreases [7].

Gas solubility is governed by its condensability and interactions with the polymer, and it is often influenced by the polymer *FFV* [7]. The *FFV* values for the amorphous phase PE analogues are calculated using Eq. (3) and density values of 0.854, 1.373, 1.660 and 2.040 g/cm^3 for PE [45], PVC [59], PVDF [60], and PTFE [61], respectively. As shown in Table 3, the CO_2 solubility increases as the δ_P increases towards 23.2 MPa$^{0.5}$, close to the solubility parameter of CO_2 (21.8 MPa$^{0.5}$), which can be explained by the regular solution theory [10]. For example, PVDF with a δ_P of 23.2 MPa$^{0.5}$ has higher CO_2 solubility than PE with a δ_P of 17.0 MPa$^{0.5}$. On the other hand, the PTFE has lower δ_P but higher CO_2 solubility than PE, which can be ascribed to the greater *FFV* in PTFE. PCTFE also shows high CO_2 solubility among these polymers, despite its relatively low values of δ_P and *FFV*.

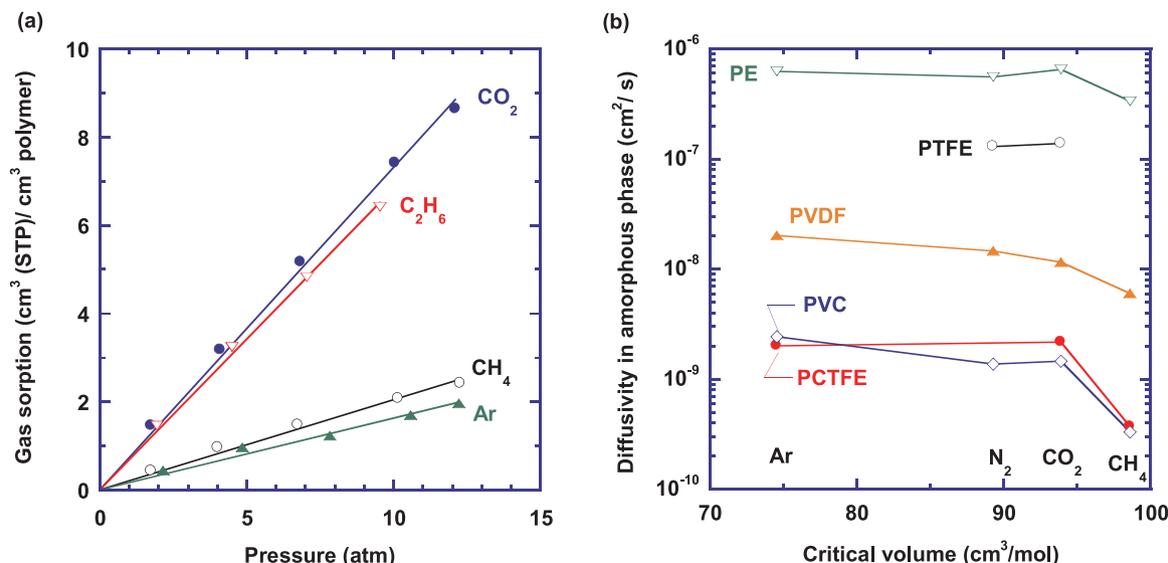Table 3 also compares gas solubility selectivity in the halogenated

Fig. 4. (a) Sorption isotherms of CH_4, Ar, C_2H_6 and CO_2 in semi-crystalline PCTFE films at 35 ˚C. The lines are the best fits based on Eq. (1). (b) Effect of penetrant critical volume on the estimated diffusivity ($D_{A,am}$) in amorphous phase polymers of PCTFE, PVC [50] and PVDF [51] at 35 ˚C, and PTFE [47] and PE [45,48] at 25 ˚C.

Table 3
Comparison of physical properties and amorphous-phase gas solubility (cm^3 (STP)/cm^3 atm) in PCTFE with PE and other halogenated PEs at 35 °C, except for PE and PTFE (25 °C).

Polymers Structure	PE [45]	PVDF [51]	PTFE [46,47]	PVC [50]	PCTFE
	H — H / H — H	F — H / F — H	F — F / F — F	H — Cl / H — H	F — Cl / F — F
φ_{am}	57% [48]	49% [51]	40% [46,47]	100% [50]	50%
T_g (°C)	−36 [53]	−40	−110 [54]	71 [55]	63
δ_P (MPa$^{0.5}$) [34]	16.2 [56]	23.2 [57]	12.7 [56]	19.8 [56]	15.7 [58]
FFV	0.191	0.156	0.215	0.165	0.170
S_{CO_2}	0.45	1.5	0.92	0.96	1.5
S_{CO_2}/S_{N_2}	11	31	7.5	26	–
S_{CO_2}/S_{Ar}	4.4	19	3.4	11	4.2
S_{CO_2}/S_{CH_4}	2.2	16	3.7	4.9	3.5

PEs. The CO_2/N_2 and CO_2/Ar solubility selectivity increases with increasing δ_P values, due to the increased CO_2 solubility. There appears no specific interactions between halogenated groups and N_2 or Ar. The CO_2/CH_4 solubility selectivity increases with increasing δ_P values and it is influenced by the F substituents, since fluoropolymers are hydrocarbon-phobic [15,23]. For example, PTFE has higher CO_2/CH_4 solubility selectivity than PE despite lower δ_P value. PCTFE exhibits higher CO_2/CH_4 solubility selectivity than PE due to the F substituents, but lower selectivity than PVC due to the lower δ_P value. Similarly, PCTFE shows a CO_2/C_2H_6 solubility selectivity of 1.1, which is much higher than PE (0.35) [45], because fluorinated polymers are hydrocarbon-phobic and thus have low C_2H_6 solubility and high CO_2/C_2H_6 solubility selectivity [15].

3.4. Effect of halogen groups on CO_2/light gas solubility selectivity

To elucidate the effect of halogen groups on CO_2/gas solubility selectivity, gas solubility data in halogenated organic liquids from the literature are used, since liquids are good markers for polymers with similar functional groups, and there are more abundant data of gas sorption in liquids than polymers. Fig. 5 shows the solubility of CO_2, Ar, N_2 and CH_4 in representative halogenated liquids with varying values of solubility parameter [62–64]. Gas solubility in liquids is often described using the regular solution theory. The CO_2 solubility is modeled using Eq. (8) [10]:

$$\ln S_{CO_2} = \ln\left(\frac{22414}{\overline{V}_{CO_2} p_{CO_2}^{sat}}\right) - \frac{\overline{V}_A (\delta_L - \delta_{CO_2})^2}{RT} \tag{8}$$

where $\overline{V}_{CO_2}$ is partial molar volume of CO_2 in organic liquids (45 cm^3/mol), $p_{CO_2}^{sat}$ is CO_2 saturation vapor pressure at 25 °C (63.4 atm), and δ_L and δ_{CO_2} are solubility parameter of the organic liquid and CO_2, respectively. As shown in Fig. 5a, the model satisfactorily describes CO_2 solubility in halogenated organic liquids with a δ_{CO_2} value of 21.8 MPa$^{0.5}$ [10].

The solubility of light gases such as N_2, Ar, and CH_4 in organic liquids can be modeled using Eq. (9) [10]:

$$\ln S_A = a + b\delta_L^2 \tag{9}$$

where a and b are adjustable constants. As shown in Fig. 5b, the b values obtained from the best fits are −0.0060, −0.0049, and −0.0029 for N_2, Ar, and CH_4, respectively.

Fig. 6a shows that the CO_2/N_2 solubility selectivity increases with increasing the δ_L values, and it is consistent with the trend in polymers. CH_2Cl_2 exhibits the highest δ_L value and thus highest CO_2/N_2 solubility selectivity among the liquids studied. Perfluorinated liquids show both lower δ_L and CO_2/N_2 solubility selectivity than hydrocarbon analogues, as indicated in C_7F_{16} and C_7H_{16}. On the other hand, asymmetric substitution using Cl increases the δ_L value and thus the CO_2/N_2 solubility selectivity, as exemplified in C_6H_5Cl and CH_2Cl_2.

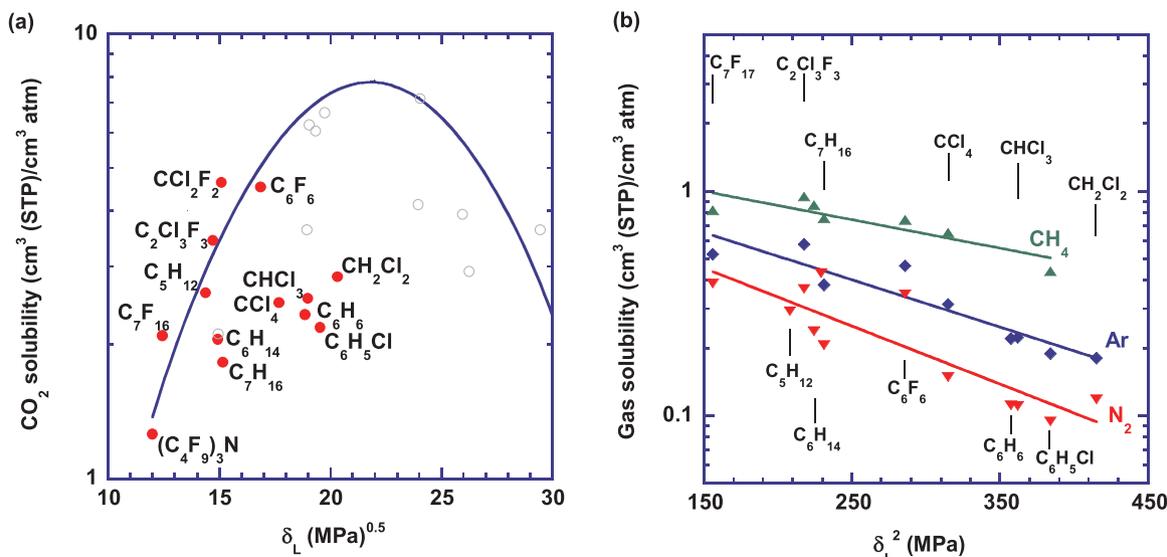Fig. 6b exhibits that CO_2/CH_4 solubility selectivity increases with

Fig. 5. Solubility of (a) CO_2 and (b) N_2, CH_4 and Ar in a variety of organic liquids including halogenated ones at about 25 °C. In (a), the symbol of ○ represents the CO_2 solubility coefficient in organic liquids from [10].
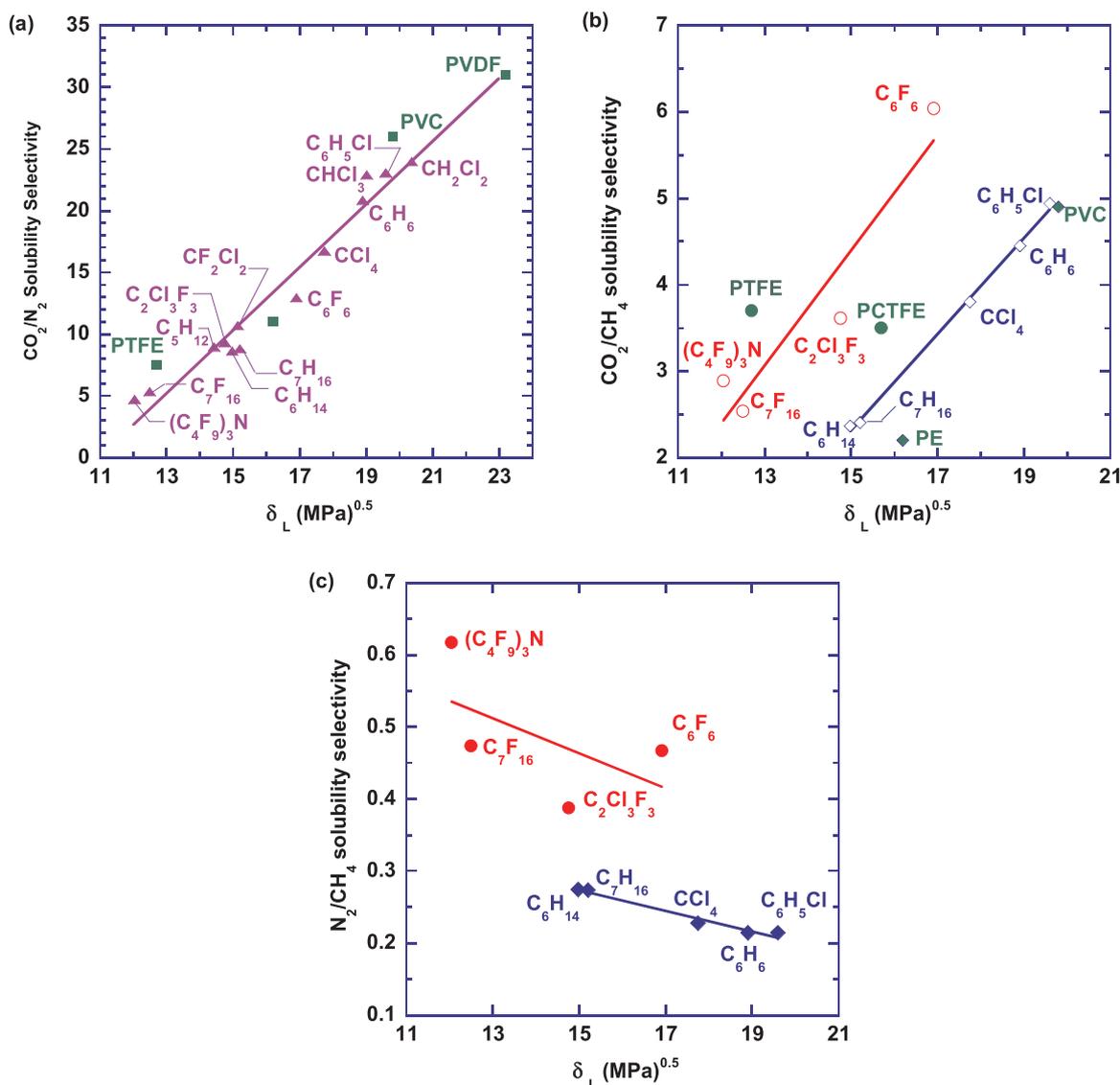
Fig. 6. Solubility selectivity of (a) CO_2/N_2, (b) CO_2/CH_4, and (c) N_2/CH_4 at ~25 °C in representative hydrocarbon and halogenated liquids with different values of solubility parameter [65,66]. Gas solubility in CH_2Cl_2 and $CHCl_3$ were taken from [64], and the data in CF_2Cl_2 are extrapolated [62,67]. The solubility in other liquids was taken from [62] for CO_2, [67] for N_2, and [68] for CH_4. The lines are to guide the eye. (For interpretation of the references to color in this figure, the reader is referred to the web version of this article.)

increasing the δ_L value. The rate of increase in CO_2/CH_4 solubility selectivity is lower than that in CO_2/N_2 solubility selectivity, partially because N_2 solubility decreases more rapidly with the δ_L value than CH_4 (cf. Fig. 5b). The fluorinated liquids show higher CO_2/CH_4 solubility selectivity than non-fluorinated ones (including hydrocarbon and chlorinated liquids), due to the unfavorable interactions between the fluorinated liquids and CH_4. These behaviors are also consistent with those in polymers, as shown in the green circles. The unfavorable interaction between fluorine and CH_4 also results in higher N_2/CH_4 solubility selectivity in fluorinated liquids than hydrocarbons and chlorinated ones, as shown in Fig. 6c.

3.5. Effect of halogen groups on noble gas/light gas solubility selectivity

Perfluoropolymers have been demonstrated to have unfavorable interactions towards H_2, but not He. For example, the He/H_2 solubility selectivity in Teflon AF1600 and Nafion is much higher than that in hydrocarbon based polymers [22]. To elucidate the effect of F and Cl on the interactions with noble gases, Fig. 7a presents He/H_2 solubility selectivity in halogenated liquids. H_2 with a T_c of 33 K is more condensable than He with a T_c of 5.2 K and thus, H_2 exhibits higher

solubility than He in liquids. For example, hydrocarbon liquids (such as pentadecane, benzene, cyclohexane, dodecane, heptane, ethanol, pentane, and hexane) show He/H_2 solubility selectivity between 0.25 and 0.40. On the other hand, the fluorinated liquids show much higher He/H_2 solubility selectivity than non-fluorinated liquids including hydrocarbons and chlorinated ones, and the δ_L value has negligible effect on the He/H_2 solubility selectivity. Fig. S2a in the Supplemental Information also shows that increasing fluorine to carbon ratio in the liquids increases He solubility.

Fig. 7b presents Ar/O_2 solubility selectivity in halogenated liquids. Ar with a T_c of 151 K has condensability similar to O_2 (with a T_c of 154 K). In contrast to He/H_2 separation, the presence of F or Cl has negligible effect of Ar/O_2 solubility selectivity, indicating the lack of any specific interactions between fluorine and Ar. Fig. S2b in the Supplemental Information also shows that increasing the F/C ratio in the liquids has no effect on the Ar solubility.

Fig. 8 shows the relative solubility (S_r) of noble gases and H_2 in various liquids to that in pentane at 25 °C. For non-fluorinated liquids including hydrocarbons and chlorinated ones, all of the gases show similar S_r values, suggesting the absence of any specific interactions. On the other hand, for fluorinated liquids, He and Ne exhibit much higher
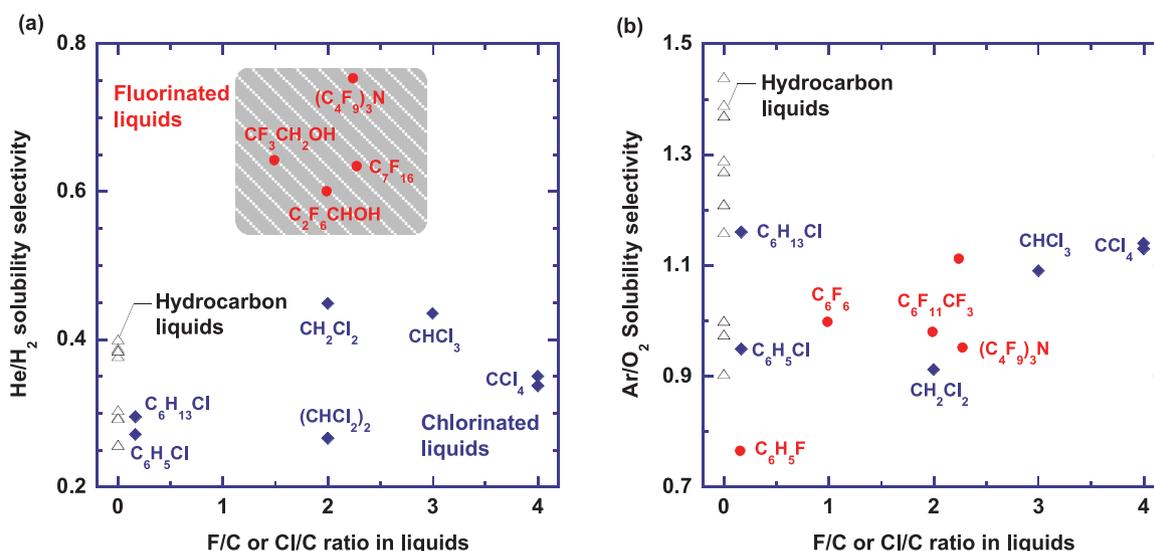
Fig. 7. (a) He/H$_2$ solubility selectivity, and (b) Ar/O$_2$ solubility selectivity at 25 °C in (Δ) hydrocarbon, (●) fluorinated and (◆) chlorinated liquids as a function of the F or Cl to carbon ratio in the liquids [64,69–72]. In (a), hydrocarbon liquids are pentadecane, benzene, cyclohexane, dodecane, heptane, ethanol, pentane and hexane in the order of increasing He/H$_2$ solubility selectivity. In (b), hydrocarbon liquids are bromobenzene, iodobenzene, benzene, methlcyclohexane, cyclohexane, hexane, heptane, dodecane, pentane and pentadecane in the order of increasing Ar/O$_2$ solubility selectivity.
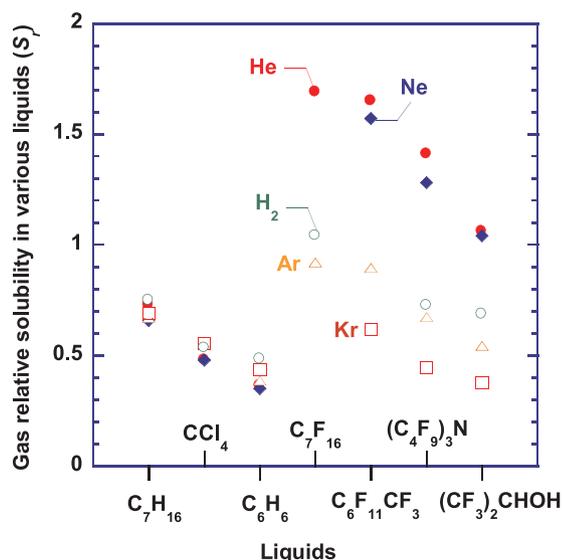

Fig. 8. Relative solubility (S_r) of He, Ne, H$_2$, Ar, and Kr in various liquids to that in pentane at 25 °C. The solubility of He, Ne, H$_2$, Ar, and Kr in pentane is 0.052 [69], 0.082 [69], 0.13 [70], 0.57 [71], and 1.6 [73] cm^3 (STP)/cm^3 atm, respectively.

S_r values than H$_2$ and other noble gases (i.e., Ar and Kr). The S_r decreases in the order of He > Ne > H$_2$ > Ar > Kr, which is similar to that for the gas polarizability values, as shown in Table 1. We suspect that the unfavorable interactions between the F substituents and gases increases with increasing the gas polarizability. Greater values of polarizability suggest that electron clouds of gas molecules can be more easily disrupted by an electric field, presumably resulting in the greater polarity and more unfavorable interactions with the C–F bonds. For example, He and Ne have much lower polarizability values than H$_2$ and therefore, the S_r values for He and Ne are much higher than H$_2$. While the concept of polarizability can satisfactorily explains the gas solubility data in Fig. 8 as well as in Fig. S3, in-depth studies of the interactions between fluorinated materials and gases will be needed to fully understand the gas solubility in these materials.

3.6. Superior gas separation performance of PCTFE

Fig. 9 demonstrates the performance of semi-crystalline PCTFE for the separation of He/H$_2$, He/CO$_2$, and H$_2$/CO$_2$ in Robeson's plots [4]. The upper bounds of He/gas separation are governed by the perfluoropolymers, due to their high He solubility [22]. The semi-crystalline PCTFE exhibits the He/gas separation performance near upper bound, suggesting the potential of this material for these applications. In particular, PCTFE shows the highest He/H$_2$ selectivity among all polymeric materials investigated. As shown in Fig. 9c, PCTFE also exhibits good H$_2$/CO$_2$ separation properties with a H$_2$/CO$_2$ selectivity of 8.8 at 35 °C.

Fig. 10 compares He/CH$_4$ and Ar/CH$_4$ separation properties in Robeson's plots for the amorphous-phase PCTFE with amorphous-phase PE analogues. PCTFE shows superior He/CH$_4$ separation property (near the upper bound), which is much better than other PE analogues such as PE, PVC and PTFE. Despite its simple chemical structure, PCTFE demonstrates its promise for He recovery from natural gas, presumably due to the unexpectedly high He solubility and unfavorable interactions towards CH$_4$. As shown in Fig. 10b, PCTFE also shows reasonably good Ar/CH$_4$ separation property, due to the unfavorable interactions with CH$_4$.

Fig. 10a also shows the effect of Cl substituent on gas separation properties, as elucidated in the comparison between PCTFE and PTFE, and between PVC and PE. PCTFE exhibits about two order of magnitude higher He/CH$_4$ selectivity than PTFE, though both polymers contain F substituents and are expected to have similar interactions with He and CH$_4$. Therefore, the difference in the gas selectivity should be derived from the difference in diffusivity selectivity. The Cl substituent increases the T_g, and thus increase size-sieving ability and He/CH$_4$ diffusivity selectivity. As shown in Table 3, PCTFE is a glassy polymer (T_g = 63 °C) while PTFE is a rubbery polymer (T_g = −110 °C). Similar behavior is also observed for PE (T_g = −36 °C) and PVC (T_g = 71 °C), both of which do not contain F. PVC shows much higher He/CH$_4$ selectivity than PE, due to the higher T_g and stronger size-sieving ability.

4. Conclusion

Despite its simple chemical structure, PCTFE demonstrates surprisingly superior He/gas separation properties due to the F and Cl substituents. The F substituents leads to unexpectedly high He solubility,
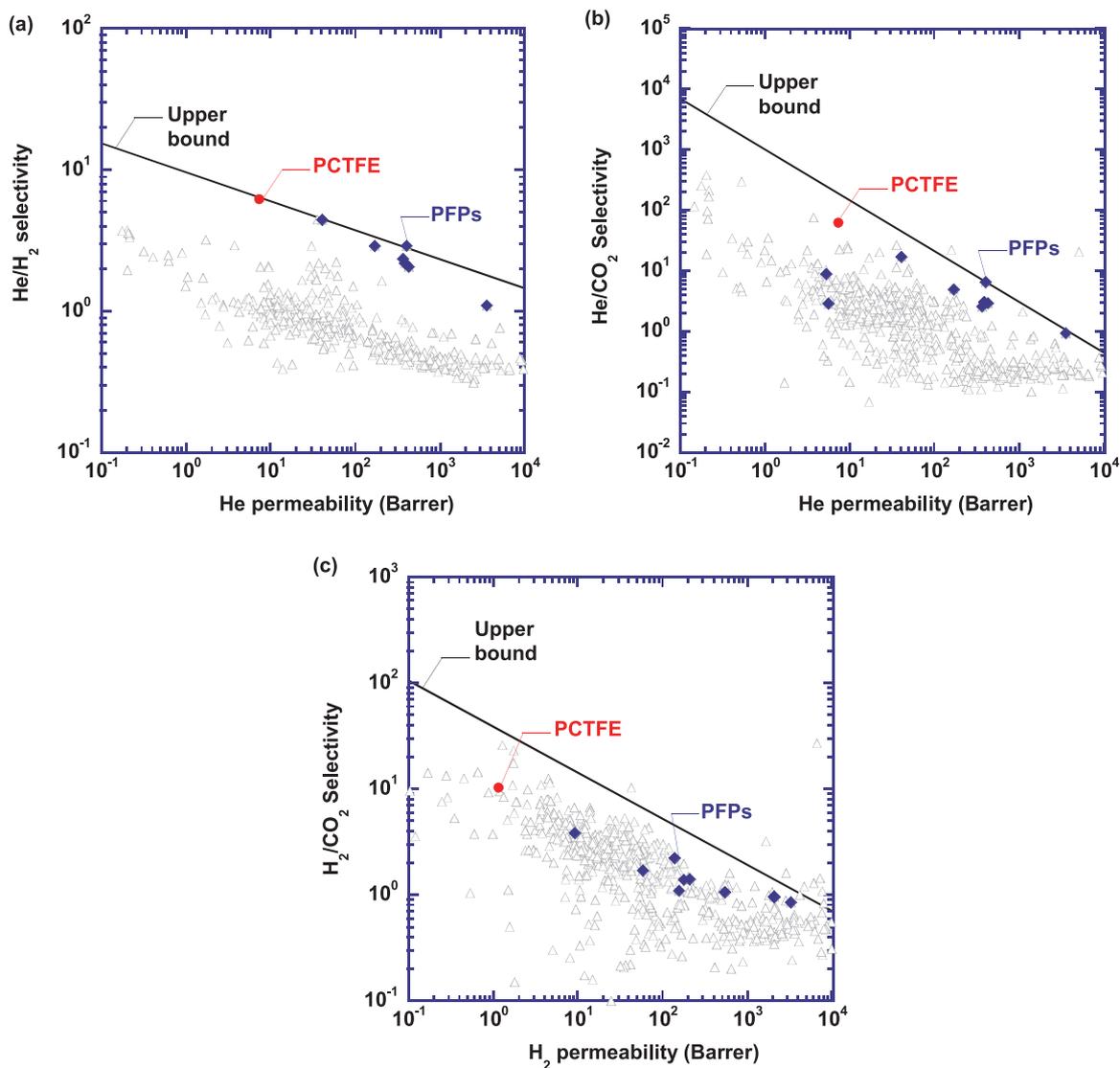
Fig. 9. Comparison of the semi-crystalline PCTFE with perfluoropolymers (PFPs) and other polymers for (a) He/H$_2$, (b) He/CO$_2$, and (c) H$_2$/CO$_2$ separation at 35 °C in the Robeson's plots [4].
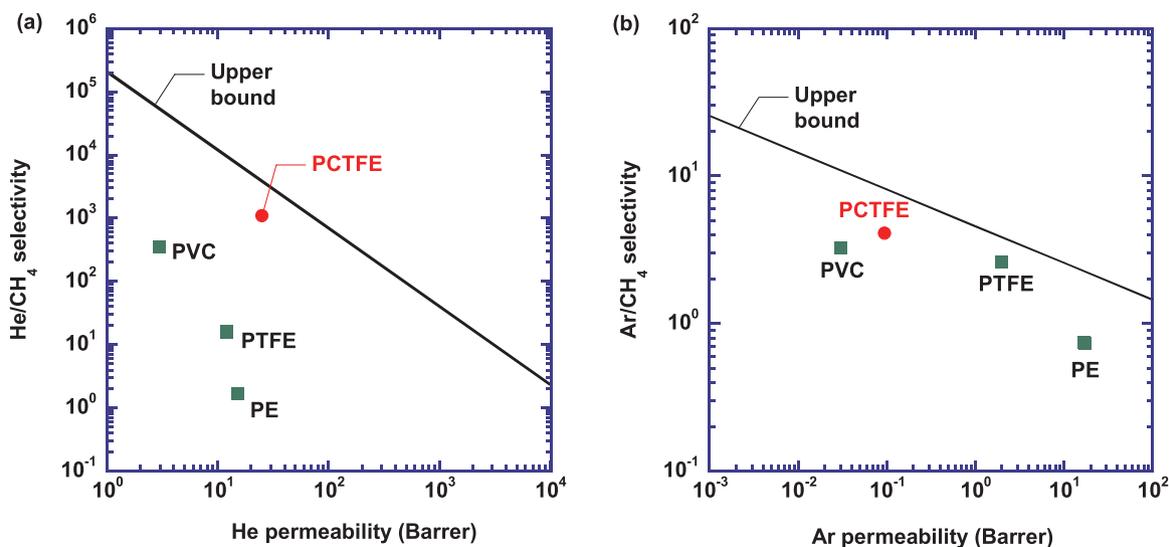

Fig. 10. Robeson's plots for (a) He/CH$_4$ and (b) Ar/CH$_4$ separation [4]. The Ar/CH$_4$ upper-bound is estimated using $\alpha_{Ar/CH_4} = \beta_{Ar/CH_4}/P_{Ar}^{\lambda_{Ar/CH_4}}$ with $\beta_{Ar/CH_4} = 0.0147$ and $\lambda_{Ar/CH_4} = 0.25$ [7]. For PE analogues including PCTFE, PVC, PTFE and PE, the amorphous phase permeability is used.

and show unfavorable interactions with H_2 and CH_4 and no specific interactions with N_2 and CO_2, leading to the superior He/gas separation properties, particularly for He/H_2 and He/CH_4 separation. Such interactions were thoroughly elucidated by evaluating the gas solubility selectivity in a variety of organic liquids including hydrocarbons and halogenated ones. Interestingly, the F containing liquids also exhibit unexpectedly high solubility for Neon, but not for Argon or Krypton.

The Cl substituents do not show any specific interactions with the gases studied, including He, H_2, N_2, CH_4, and Ar. On the other hand, the asymmetric substitution of Cl increases solubility parameter and T_g in the polymers, increasing size-sieving ability. Since the He has the smallest molecular size among the penetrants studied, the Cl substituents in PCTFE yields high He/gas diffusivity selectivity, which leads to the superior He/gas selectivity when coupled with good He/gas solubility selectivity.

Acknowledgments

Appendix A. Supplementary material

Supplementary data associated with this article can be found in the online version at http://dx.doi.org/10.1016/j.memsci.2017.11.043.

References

[1] R.W. Baker, B.T. Low, Gas separation membrane materials: a perspective, Macromolecules 47 (2014) 6999–7013.

[2] H. Lin, Integrated membrane material and process development for gas separation, Curr. Opin. Chem. Eng. 4 (2014) 54–61.

[3] D.F. Sanders, Z.P. Smith, R. Guo, L.M. Robeson, J.E. McGrath, D.R. Paul, B.D. Freeman, Energy-efficient polymeric gas separation membranes for a sustainable future: a review, Polymer 54 (2013) 4729–4761.

[4] L.M. Robeson, The upper bound revisited, J. Membr. Sci. 320 (2008) 390–400.

[5] L.M. Robeson, Z.P. Smith, B.D. Freeman, D.R. Paul, Contributions of diffusion and solubility selectivity to the upper bound analysis for glassy gas separation membranes, J. Membr. Sci. 453 (2014) 71–83.

[6] H.B. Park, J. Kamcev, L.M. Robeson, M. Elimelech, B.D. Freeman, Maximizing the right stuff: the trade-off between membrane permeability and selectivity, Science 356 (2017).

[7] B.D. Freeman, Basis of permeability/selectivity tradeoff relations in polymeric gas separation membranes, Macromolecules 32 (1999) 375–380.

[8] H. Lin, M. Yavari, Upper bound of polymeric membranes for mixed-gas CO_2/CH_4 separations, J. Membr. Sci. 475 (2015) 101–109.

[9] H. Lin, E. Van Wagner, B.D. Freeman, L.G. Toy, R.P. Gupta, Plasticization-enhanced H_2 purification using polymeric membranes, Science 311 (2006) 639–642.

[10] H. Lin, B.D. Freeman, Materials selection guidelines for membranes that remove CO_2 from gas mixtures, J. Mol. Struct. 739 (2005) 57–74.

[11] N.Y. Du, H.B. Park, G.P. Robertson, M.M. Dal-Cin, T. Visser, L. Scoles, M.D. Guiver, Polymer nanosieve membranes for CO_2-capture applications, Nat. Mater. 10 (2011) 372–375.

[12] J. Liu, X. Hou, H. Park, H. Lin, High performance polymers for membrane CO_2/N_2 separation, Chem. Eur. J. 22 (2016) 15980–15990.

[13] M.R. Pixton, D.R. Paul, Gas transport properties of polyarylates part II: Tetrabromnation of the bisphenol, J. Polym. Sci. Part B: Polym. Phys. 33 (1995) 1353–1364.

[14] T.C. Merkel, V. Bondar, K. Nagai, B.D. Freeman, Y.P. Yampolskii, Gas sorption, diffusion, and permeation in poly(2,2-bis(trifluoromethyl) − 4,5-difluoro-1,3-dioxole-co-tetrafluoroethylene), Macromolecules 32 (1999) 8427–8440.

[15] R.S. Prabhakar, B.D. Freeman, I. Roman, Gas and vapor sorption and permeation in poly(2,2,4-trifluoro-5-trifluoromethoxy-1,3-dioxole-co-tetrafluoroethylene), Macromolecules 37 (2004) 7688–7697.

[16] R.S. Prabhakar, T.C. Merkel, B.D. Freeman, T. Imizu, A. Higuchi, Sorption and transport properties of propane and perfluoropropane in poly(dimethylsiloxane) and poly(1-trimethylsilyl-1-propyne), Macromolecules 38 (2005) 1899–1910.

[17] M. Mukaddam, E. Litwiller, I. Pinnau, Gas sorption, diffusion, and permeation in Nafion, Macromolecules 49 (2016) 280–286.

[18] M.S. McCaig, E.D. Seo, D.R. Paul, Effects of bromine substitution on the physical and gas transport properties of five series of glassy polymers, Polymer 40 (1999) 3367–3382.

[19] R. Nikiforov, N. Belov, A. Zharov, I. Konovalova, B. Shklyaruk, Y. Yampolsky, Gas permeation and diffusion in copolymers of tetrafluoroethylene and

[20] hexafluoropropylene: effect of annealing, J. Membr. Sci. 540 (2017) 129–135.

[20] Y. Okamoto, Q.M. Du, K. Koike, F. Mikes, T.C. Merkel, Z.J. He, H. Zhang, Y. Koike, New amorphous perfluoro polymers: perfluorodioxolane polymers for use as plastic optical fibers and gas separation membranes, Polym. Adv. Technol. 27 (2016) 33–41.

[21] Y. Okamoto, H. Zhang, F. Mikes, Y. Koike, Z.J. He, T.C. Merkel, New perfluorodioxolane-based membranes for gas separations, J. Membr. Sci. 471 (2014) 412–419.

[22] Z.P. Smith, R.R. Tiwari, M.E. Dose, K.L. Gleason, T.M. Murphy, D.F. Sanders, G. Gunawan, L.M. Robeson, D.R. Paul, B.D. Freeman, Influence of diffusivity and sorption on helium and hydrogen separations in hydrocarbon, silicon, and fluorocarbon-based polymers, Macromolecules 47 (2014) 3170–3184.

[23] T.C. Merkel, I. Pinnau, R. Prabhakar, B.D. Freeman, Gas and vapor transport properties of perfluoropolymers, in: B.D. Freeman, Y. Yampolski, I. Pinnau (Eds.), Materials Science of Membranes for Gas and Vapor Separation, John Wiley & Sons, Ltd., West Sussex, England, 2006.

[24] M. Fang, Y. Okamoto, Y. Koike, Z. He, T.C. Merkel, Gas separation membranes prepared with copolymers of perfluoro(2-methylene-4,5-dimethyl-1,3-dioxlane) and chlorotrifluoroethylene, J. Fluor. Chem. 188 (2016) 18–22.

[25] R. Waack, N.H. Alex, H.L. Frisch, V. Stannett, M. Szwarc, Permeability of polymer films to gases and vapors, Ind. Eng. Chem. 47 (1955) 2524–2527.

[26] H. Lin, B. Freeman, Permeation and diffusion, in: H. Czichos, L.E. Smith, T. Saito (Eds.), Springer-Handbook of Materials Measurement Methods, Springer, Leipzig, 2006, pp. 371–387.

[27] M. Yavari, S.H. Maruf, Y.F. Ding, H. Lin, Physical aging of glassy perfluoropolymers in thin film composite membranes. Part II. Glass transition temperature and the free volume model, J. Membr. Sci. 525 (2017) 399–408.

[28] H. Lin, B.D. Freeman, Gas solubility, diffusivity and permeability in poly(ethylene oxide), J. Membr. Sci. 239 (2004) 105–117.

[29] P.R. Bevington, D.K. Robinson, Data Reduction and Error Analysis for the Physical Sciences, 2nd ed, McGraw-Hill, Inc, New York, 1992.

[30] J.G. Wijmans, R.W. Baker, The solution-diffusion model: a review, J. Membr. Sci. 107 (1995) 1–21.

[31] J.K. Park, D.R. Paul, Correlation and prediction of gas permeability in glassy polymer membrane materials via a modified free volume based group contribution method, J. Membr. Sci. 125 (1997) 23–39.

[32] H. Lin, E. Van Wagner, S.J. Swinnea, B.D. Freeman, S.J. Pas, A.J. Hill, S. Kalakkunnath, D.S. Kalika, Transport and structural characteristics of crosslinked poly(ethylene oxide) rubbers, J. Membr. Sci. 276 (2006) 145–161.

[33] K.A. O'Leary, D.R. Paul, Physical properties of poly(n-alkyl acrylate) copolymers. Part 1. Crystalline/crystalline combination, Polymer 47 (2006) 1226–1244.

[34] D.W. Van Krevelen, K. Te Nijenhuis, Properties of Polymers: Their Correlation with Chemical Structure; Their Numerical Estimation and Prediction from Additive group Contributions, Elsevier, Amsterdam, 2009.

[35] N.S. Murthy, Y.P. Khanna, A.J. Signorelli, Crystallinities of poly(chlorotrifluoroethylene) and its copolymers by differential scanning calorimetry, X-ray diffraction, and density measurements, Polym. Eng. Sci. 34 (1994) 1254–1259.

[36] J.D. Hoffman, G. Williams, E. Passaglia, Analysis of the α, β, and γ relaxations in polychlorotrifluoroethylene and polyethylene: dielectric and mechanical properties, J. Polym. Sci. Part C: Polym. Symp. 14 (1966) 173–235.

[37] R.J. Graves, H.W. White, Specific heat of halocarbon 25–5 s grease (polychlorotrifluoroethylene in silica gel) below 4.5 K, Cryogenics 20 (1980) 525–526.

[38] S.-S. Chang, J. Weeks, Heat capacity and thermodynamic properties of poly (chlorotrifluoroethylene) from 2.5 to 620 k, J. Res. Natl. Inst. Stand. Technol. 97 (1992) 341–363.

[39] S. Sunderrajan, B.D. Freeman, C.K. Hall, I. Pinnau, Propane and propylene sorption in solid polymer electrolytes based on poly(ethylene oxide) and silver salts, J. Membr. Sci. 182 (2001) 1–12.

[40] N.S. Murthy, H. Minor, Analysis of poorly crystallized polymers using resolution enhanced X-ray diffraction scans, Polymer 36 (1995) 2499–2504.

[41] J. Chiou, J.W. Barlow, D. Paul, Plasticization of glassy polymers by CO_2, J. Appl. Polym. Sci. 30 (1985) 2633–2642.

[42] J. Brandrup, E.H. Immergut, E.A. Grulke, Polymer Handbook, 3rd ed, Wiley, New York, 1989.

[43] A.W. Myers, V. Tammela, V. Stannett, M. Szwarc, Permeability of chlorotrifluoroethylene polymers, Mod. Plast. 37 (1960) 139–140.

[44] J.R. Rumble, CRC Handbook of Chemistry and Physics, CRC Press/Taylor & Francis, Boca Raton, FL, 2018 98th (Internet Version) ed..

[45] A.S. Michaels, H.J. Bixler, Solubility of gases in polyethylene, J. Polym. Sci. 50 (1961) 393–412.

[46] M. Matsuyama, H. Miyake, K. Ashida, K. Watanabe, Permeation, diffusion and dissolution of hydrogen isotopes, methane and inert-gases through in a tetrafluoroethylene film, J. Nucl. Mater. 110 (1982) 296–300.

[47] R.A. Pasternak, M.V. Christensen, J. Heller, Diffusion and permeation of oxygen, nitrogen, carbon dioxide, and nitrogen dioxide through polytetrafluoroethylene, Macromolecules 3 (1970) 366–371.

[48] A.S. Michaels, H.J. Bixler, Flow of gases through polyethylene, J. Polym. Sci. 50 (1961) 413–439.

[49] W.J. Koros, D.R. Paul, CO_2 sorption in poly(ethylene terephthalate) above and below the glass transition, J. Polym. Sci., Polym. Phys. Ed. 16 (1978) 1947–1963.

[50] M.J. El-Hibri, D.R. Paul, Effects of uniaxial drawing and heat-treatment on gas sorption and transport in PVC, J. Appl. Polym. Sci. 30 (1985) 3649–3678.

[51] M.J. El-Hibri, D.R. Paul, Gas transport in poly(vinylidene fluoride): effects of uniaxial drawing and processing temperature, J. Appl. Polym. Sci. 31 (1986) 2533–2560.

[52] J.M. Mohr, D.R. Paul, Comparison of gas permeation in vinyl and vinylidene

polymers, J. Appl. Polym. Sci. 42 (1991) 1711–1720.

[53] U. Gaur, B. Wunderlich, Heat capacity and other thermodynamic properties of linear macromolecules. II. Polyethylene, J. Phys. Chem. Ref. Data 10 (1981) 119–152.

[54] G. Calleja, A. Jourdan, B. Ameduri, J.-P. Habas, Where is the glass transition temperature of poly(tetrafluoroethylene)? A new approach by dynamic rheometry and mechanical tests, Eur. Polym. J. 49 (2013) 2214–2222.

[55] M.J. Elhibri, D.R. Paul, Effects of uniaxial drawing and heat-treatment on gas sorption and transport in PVC, J. Appl. Polym. Sci. 30 (1985) 3649–3678.

[56] J. Brandrup, E.H. Immergut, Polymer Handbook, John Wiley & Sons, New York, 1990.

[57] A. Bottino, G. Capannelli, S. Munari, A. Turturro, Solubility parameters of poly (vinylidene fluoride), J. Polym. Sci. Part B: Polym. Phys. 26 (1988) 785–794.

[58] A.F.M. Barton, Handbook of Polymer-liquid Interaction Parameters and Solubility Parameters, CRC Press, New York, 1990.

[59] G. Wypych, PVC Degradation and Stabilization, Third ed., ChemTec Publishing, Boston, 2015.

[60] K. Nakagawa, Y. Ishida, Estimation of amorphous specific volume of poly(vinylidene fluoride) as a function of temperature, Colloid Polym. Sci. 251 (1973) 103–107.

[61] H.W. Starkweather, The density of amorphous polytetrafluoroethylene, J. Polym. Sci. Part B: Polym. Phys. 20 (1982) 2159–2161.

[62] P.G. Fogg, IUPAC Solubility Data Series: Carbon Dioxide in Non-aqueous Solvents at Pressures less than 200 kpa, Pergamon Press, New York, 1992.

[63] R. Battino, T.R. Rettich, T. Tominaga, The solubility of nitrogen and air in liquids, J.

Phys. Chem. Ref. Data 13 (1984) 563–600.

[64] K. Shirono, T. Morimatsu, F. Takemura, Gas solubilities (CO_2, O_2, Ar, N_2, H_2, and He) in liquid chlorinated methanes, J. Chem. Eng. Data 53 (2008) 1867–1871.

[65] E.P. Bruce, M.P. John, P.O.C. John, Fluid phase equilibria in multicomponent systems, in: Properties of Gases and Liquid, Fifth edition, McGraw Hill Professional, New York, 2001.

[66] C.L. Yaws, K.Y. Li, Chapter 13 - Solubility Parameter and Liquid Volume—Organic Compounds, in: Thermophysical Properties of Chemicals and Hydrocarbons, William Andrew Publishing, Norwich, NY, 2009, pp. 597–643.

[67] H.L. Clever, R. Battino, H. Miyamoto, Y. Yampolski, C.L. Young, IUPAC-NIST solubility data series. 103. Oxygen and ozone in water, aqueous solutions, and organic liquids (Supplement to Solubility Data Series Volume 7), J. Phys. Chem. Ref. Data 43 (2014) 033102.

[68] H.L. Clever, C.L. Young, IUPAC Solubility Data Series: Methane, Pergamon Press, New York, 1987.

[69] H.L. Clever, IUPAC Solubility Data Series: Helium and Neon, Pergamon Press, New York, 1979.

[70] C.L. Young, IUPAC Solubility Data Series: Hydrogen and Deuterium, Pergamon Press, New York, 1981.

[71] H.L. Clever, IUPAC Solubility Data Series: Argon, Pergamon Press, New York, 1980.

[72] R. Battino, IUPAC Solubility Data Series: Oxygen and Ozone, Pergamon Press, New York, 1981.

[73] H.L. Clever, IUPAC Solubility Data Series: Krypton, Xenon and Radon, Pergamon Press, New York, 1979.